Bull Earthquake Eng (2013) 11:2309–2332
DOI 10.1007/s10518-013-9479-7

ORIGINAL RESEARCH PAPER

Seismic behavior of viscously damped yielding frames under structural and damping uncertainties

O. Lavan · M. Avishur

Received: 31 December 2012 / Accepted: 23 June 2013 / Published online: 5 July 2013

Abstract This paper examines the sensitivity of the response of optimally damped frames to uncertainty in structural and damping properties. Viscous dampers are first optimally designed for given nominal properties of the retrofitted structures and a given ensemble of records for each structure. The behavior of the retrofitted structures (in terms of the maximum envelope peak inter-story drift) considering uncertainty in their properties as well as in the dampers' properties is then tested using Monte Carlo simulation. It is shown that the uncertainties lead to larger mean drifts than expected, and that some designs are more sensitive than others. The physical reasons for this behavior are discussed and some rules as to what designs are expected to be more sensitive are given.

Keywords Seismic retrofitting · Passive control · Viscous dampers · Fully stressed design

1 Introduction

Over the past two decades there has been a significant shift in the approach to seismic design. Many new technologies associated with passive energy dissipation and control have been introduced and have reached a considerable level of maturity (e.g. Soong and Dargush 1997; Christopoulos and Filiatrault 2006; Takewaki 2009). Of these, viscous dampers seem to have some performance advantage as the forces they produce are out of phase with displacement–induced forces in the structure (Constantinou and Symans 1992). Hence, viscous dampers are dealt with in this paper. In addition to the maturity of passive energy dissipation technologies, the overall concept of performance-based design has gained prominence. These developments have increased the motivation for seismic retrofitting. However, as a result, the design process itself has become increasingly complex. Consequently, design including optimization of

O. Lavan (✉) · M. Avishur
Faculty of Civil and Environmental Engineering, Technion—Israel Institute of Technology, Technion City, 32000 Haifa, Israel
e-mail: lavan@tx.technion.ac.il

M. Avishur
e-mail: meiri@gash.co.il

seismic retrofit solutions using viscous dampers has also been studied extensively (Agrawal and Yang 1999; Attard 2007; Aydin et al. 2007; Cheng and Pantelides 1988; Dargush and Sant 2005; Fujita et al. 2010; Gluck et al. 1996; Hwang et al. 2008; Kim et al. 2003; Lavan and Dargush 2009; Lavan and Levy 2005, 2006, 2009; Levy and Lavan 2006, 2009; Liu et al. 2005; Lopez Garcia and Soong 2002; Park et al. 2004; Shukla and Datta 1999; Silvestri and Trombetti 2007; Singh and Moreschi 2001, 2002; Takewaki 1997; Trombetti and Silvestri 2007; Wu et al. 1997; Yang et al. 2002; Zhang and Soong 1992). Optimal design has matured to such a level that in some cases even simple design tools for practicing engineers have been supplied (Lopez Garcia and Soong 2002; Levy and Lavan 2006).

The aforementioned retrofit solution methodologies have matured to the extent of considering also some uncertainty in the earthquake hazard characterization. This is done by adopting either an ensemble of records that were selected and scaled using statistical tools, or using a stochastic process, to represent the seismic hazard. Uncertainty in soil properties can also be easily accounted for in the design. The number of parameters controlling soil behavior is very small and their effect on responses of interest is usually monotonic. Thus, ”conservative assumptions” can easily be made by using minimum and maximum values for those parameters. For prediction of the behavior of a structure, while considering soil-structure interaction and uncertainty in soil properties only, the analysis is to be repeated for several combinations of the limit values of soil parameters. Nonetheless, not more than two analyses would usually be required in this case. Such a limit analysis can easily be executed during the design process itself. This would lead to more robust designs. On the other hand, if uncertainty in structural properties is to be considered, the number of such properties may be very large. Additionally, their effect on various responses of interest may be conflicting. That is, a ”conservative assumption” made for one response (e.g. drift of the story i) may not be conservative for the other (e.g. drift of the story $j \neq i$). Thus, if such uncertainty is to be considered using a limit analysis, many dynamic analyses would be required. Moreover, when considering uncertainty through a limit analysis the probability that, simultaneously, all parameters attain their values that lead to the worse response reduces with the number of parameters. Hence, considering the effect of uncertainty in the structural properties through a limit analysis may lead to very conservative designs. In view of the above, most available design procedures make use of nominal values for the properties of the structure to be retrofitted. It should be emphasized that the distribution of viscous dampers has a major effect on its seismic performance (e.g. Hahn and Sathiavageeswaran 1992). This highlights the importance of optimization. Nonetheless, in many cases optimal designs may be very sensitive to uncertainties in the problem parameters. Hence, it is important to evaluate a solution’s sensitivity to such uncertainty. It should be noted that, in case of retrofitting, this uncertainty is expected to be more pronounced and is strongly dependent on the documentation available. In this study, it is assumed that the layout of the structure is known and that documentation in the form of construction plans is available. The uncertainty is limited to dimensions and material properties.

It should be noted that methodologies for the seismic design of energy dissipation systems while accounting for structural uncertainties have been proposed. Takewaki and Ben-Haim (2005) applied concepts from the Info-Gap Theory (Ben-Haim 2001) and formulated a design concept that maximizes the robustness of the system while satisficing the performance requirements. Taflanidis and Beck (2008) proposed an optimal design procedure considering uncertainty and applied it to the design of base isolated structures. Dargush and Sant (2005) indicated that structural uncertainties could be accounted for in their genetic algorithm framework. While presenting a huge step forward, these require advanced tools from optimization and/or reliability analysis as well as a vast computational effort. In addition,

sometimes a small compromise on the limits assigned by the constraints of the optimization problem, which are related to the performance of the structure, is not fatal. Moreover, sometimes the responses of interest are not expected to be very sensitive to uncertainty in structural properties. From a practical point of view, in such cases the use of such tools may be avoided. While the engineer knows in advance if some compromise on the performance of the structure is acceptable the sensitivity of the response to uncertainty is unknown, and is the subject of this paper.

One approach for assessing the effect of uncertainty, that is adopted in this paper, makes use of Monte Carlo simulation. Monte Carlo simulation has been used in the context of energy dissipation devices for seismic applications. Di Paola et al. made use of such a simulation to validate expressions they proposed for equivalent linear viscous damping of SDOF (Di Paola et al. 2007) as well as MDOF (Di Paola and Navarra 2009) systems equipped with nonlinear viscous dampers. Monte Carlo simulations were also used by Politopoulos et al. to assess the vulnerability of base isolated structures considering uncertainties in the ground motion and the structural properties. In an early study (Politopoulos and Sollogoub 2005), the vulnerability of structures isolated using rubber bearings was compared to that of conventional structures. They modeled the superstructure as an elastoplastic SDOF system. Later on, Politopoulos and Pham (2009) extended this study to account for various types of bearings and hysteretic models for the super structure. It should be noted that other methods have been developed for this purpose (see e.g. Fujita and Takewaki 2012)

This paper examines the sensitivity of the response of optimally damped yielding frames to uncertainty in structural and damping properties. This will allow engineers to optimally design the seismic retrofitting by means of viscous dampers using simple available methodologies while having insight on the order of magnitude of the sensitivity of the attained designs to structural uncertainties. Viscous dampers are first optimally designed for the nominal properties of the retrofitted structures and given ensembles of records. Note that in the framework of performance-based-design (PBD) damped structures could yield under the strongest level of ground motions considered. Hence, yielding frames with various allowable inter-story drifts, some are relatively high for the design basis earthquake, are considered. The behavior of the damped structures considering uncertainty in their properties and in the dampers' properties is then tested using Monte Carlo simulation. Six frames are considered in this study: three yielding shear frames, two flexural RC frames and a flexural steel frame. The following section describes the optimization problem considered and the methodology to be used for evaluating the sensitivity to uncertainty. Then, the shear frames are described along with their optimal viscous damping design and the study on their behavior under uncertainty. A similar study is then presented for the flexural frames. Finally, the conclusions of this study are summarized.

2 Methodology

2.1 General

The methodology used for evaluating the sensitivity of seismic retrofit designs to uncertainty in structural and damping properties consists of two main stages. In stage I, optimal designs of added viscous dampers are generated based on the nominal properties of the structures. In stage II, use is made of Monte Carlo simulations to assess the sensitivity of the designs to uncertainty in structural and damping properties. These two stages are presented in Fig. 1 and will be explained in detail in Sects. 2.2 and 2.3.

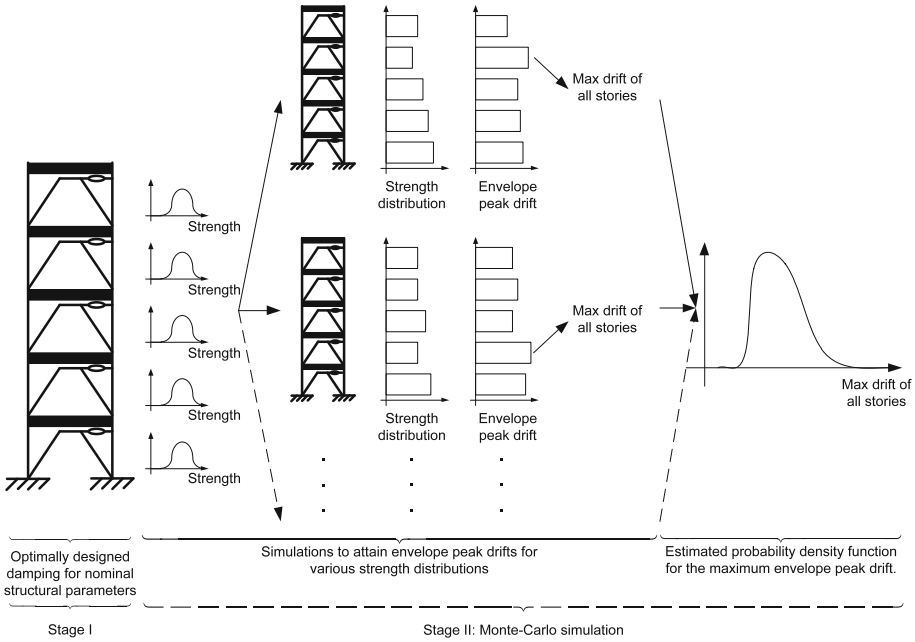

Fig. 1 Illustration of the two stages comprising the methodology

2.2 Stage I: optimization problem and procedure

This section describes the optimization problem considered as well as the procedure adopted for its solution.

2.2.1 Design variables

Viscous fluid dampers dissipate energy by means of fluid flow. They usually consist of a sealed cylinder filled with silicon oil which is forced to flow through an orifice by the action of a steel piston rod with a bronze head. The relative velocity between the ends of the damper moves the piston which forces the oil through the orifice. To fully utilize the efficiency of these dampers, they are usually attached to structures using stiff braces (Chen and Chai 2011). Hence, their behavior can be approximated mathematically as follows:

$$P(t) = c_d \text{sign}(v(t))(|(v(t)|)^{\alpha} \tag{1}$$

where P = damping force as a function of time, t v = relative velocity between the ends of the damper; c_d = zero frequency damping coefficient; sign() = the sign function, and α is an exponent. Linear viscous dampers, for which $\alpha = 1.0$, produce forces that are out-of-phase with restoring forces due to displacements. Hence, this type of damper lessens the need for column and foundation strengthening (Constantinou and Symans 1992), and is considered in this work. As the damper forces of linear viscous dampers depend linearly on the damper velocities, the sizes (damping coefficients) and locations of the dampers are the only design variables remaining. In many optimization schemes potential damper locations are predetermined. The optimization algorithm then specifies damping coefficients equal to zero in locations where dampers are not required.

2.2.2 Design objectives

Peak inter-story drifts have long been recognized as the main seismic performance measure of building structures. Hence, reduction of inter-story drifts has been adopted as a design objective in many retrofitting methodologies. Many of those methodologies adopted (or implied the adoption of) the maximum inter-story drift of all stories as their design objective (e.g. Agrawal and Yang 1999; Attard 2007; Fujita et al. 2010; Lavan and Levy 2005; Lavan and Levy 2006; Liu et al. 2005; Lopez Garcia and Soong 2002; Zhang and Soong 1992 and the comparative study by Whittle et al. (2012)). A major advantage of such design objective is its suitability to irregular structures. This is because this methodology practically considers each inter-story drift individually rather than using a smeared measure over the various stories such as an average value (Levy and Lavan 2009). Hence, the chosen performance measure in this study was the maximum envelope peak inter-story drift (MEPISD). The maximum is taken over all stories, the envelope is taken from all ground motion records in the ensemble and the peak represents the maximum of the absolute value in time. This is equivalent to constraining the envelope peak inter-story drift of each story separately in the optimization problem.

In the design of retrofitting, monetary cost usually also plays an important role. The cost of each damper is a function of three main parameters: the maximum damper force, the damper stroke and the damping coefficient. As the inter-story drifts serve as the performance measure, the damper stroke is already indirectly accounted for. When dampers are mounted between adjacent floors the damping force depends on the inter-story velocity and the damping coefficient. Assuming the response is dominated by a single mode of vibration (usually the structure's fundamental mode) having similar peak drifts in all damped stories (which reflects the drift design objective), the peak inter-story velocities in the damped stories will also be similar. Hence, taking the sum of damping coefficients as an objective is similar to taking the sum of peak damping forces. Thus, in this work, the total added damping is chosen to represent a solution's monetary cost. Note that the number of dampers also plays an important role in the cost of retrofitting. As evidenced in the aforementioned studies, the optimization problem considered below is also likely to reduce the number of dampers required.

2.2.3 Optimization problem

Based on the previous discussion, the optimization problem is to minimize the total damping added to the structure while a constraint is assigned to the envelope peak inter-story drift of each story separately. That is, envelope (for all ground motions) peak inter-story drifts are constrained. Equivalently, the constraint can be applied to the MEPISD. Formally, this optimization problem may be stated as:

$$\begin{aligned} &\text{mininimize: } J = \mathbf{c}_{\mathrm{d}}^{\mathrm{T}} \cdot \mathbf{1} \\ &\text{subject to:} \\ &pi_i = \max_t \left(|d_i(t)| / d_{all,i} \right) \leq 1.0 \, \forall i, \forall \mathbf{a}_{\mathrm{g}} \in ensemble \\ &0 \leq \mathbf{c}_{\mathrm{d}} \end{aligned} \tag{2}$$

where $\mathbf{c}_{\mathrm{d}}$ = added damping vector; d_i = inter-story drift of the ith story that is evaluated using the equations of motion for a given ensemble of ground motions; $d_{all,i}$ = the allowable value of the inter-story drift of the ith story and $\mathbf{a}_g$ = ground acceleration vector.

2.2.4 Design procedure

The optimization problem presented in the previous section has been solved by Lavan and Levy using a first order optimization approach (e.g. Lavan and Levy 2006). Later on, they formulated optimality criteria based on observed fully stressed characteristics of attained optimal designs (Levy and Lavan 2006). The fully stressed characteristics state that: *The optimal added damping is characterized by assigning added dampers only to stories that reached the allowable inter-story drift.* They further successfully targeted these fully stressed characteristics by proposing a simple analysis/redesign scheme. The analysis/redesign scheme will be used here to obtain the optimal design of dampers based on the nominal properties of the structure.

2.3 Stage II: Monte–Carlo simulation

Once an optimal design is attained based on the nominal properties of the structure, use is made of Monte Carlo simulation to assess its sensitivity to uncertainty in structural properties. That is, based on the probability distributions of the stochastic variables considered, a population of retrofitted structures is generated. Each individual frame in this population, having different structural properties, is then analyzed using the same ensemble of ground motions originally considered for design. The MEPISD is extracted from the analyses of each individual frame. In turn, the statistics of this response from all individuals is analyzed. This process is summarized in Fig. 1.

3 Case studies

3.1 General

As a preliminary study, yielding shear frames are first adopted. Shear frames usually do not adequately represent realistic frames. However, column yielding may be reasonable in cases of old framed structures that were not designed by the strong column weak beam strategy. Shear frames would also easily allow forming a weak story structure to examine its effect on the response considering uncertainty. Furthermore, sensitivity is more pronounced in shear frames thus the parameters controlling it could be more easily identified. This could facilitate the drawing of conclusions. These conclusions can then be thoroughly examined in realistic buildings, which will also be done subsequently. Finally, the following Monte Carlo simulation requires a large number of function evaluations, that is, a large number of nonlinear time history analyses. The use of shear frames for the preliminary study appreciably reduces the computational effort.

3.2 Shear frames

3.2.1 Details of the bare frames, their modeling and analysis tools

Three shear frames are considered in this study: two regular and one with a weak first story. These are now described.

The regular five-story yielding shear frame in Fig. 2a, adopted from Lavan and Dargush (2009), is the first to be considered (termed "Regular"). Here k_i is the story shear stiffness, i.e. story shear corresponding to a unit inter-story drift, Fy_i is the story yield shear force, dy_i

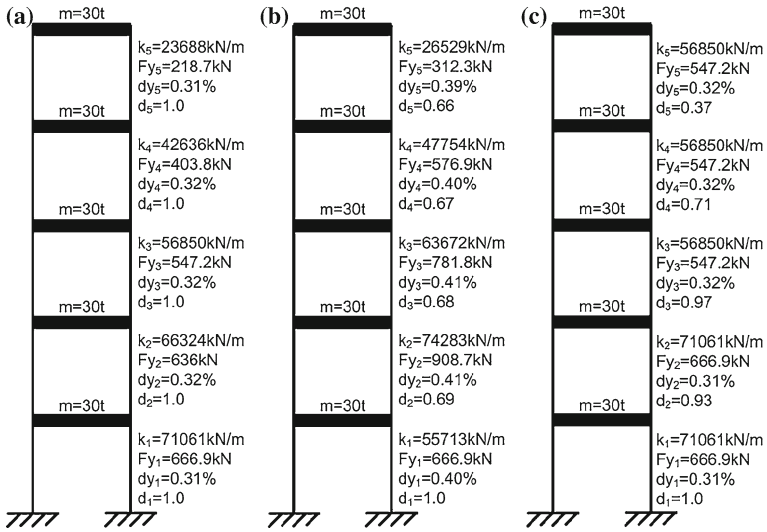

Fig. 2 **a** "Regular" **b** "Irregular", and **c** "Regular2" shear frames

Table 1 Ground motions' parameters

SAC name	Record	Earthquake magnitude	Distance (km)	Scale factor	Duration (s)	PGA (cm/s^2)
LA04	Imperial valley, 1979, array #05	6.5	4.1	1.01	39.38	478.65
LA06	Imperial valley, 1979, array #06	6.5	1.2	0.84	39.08	230.08
LA07	Landers, 1992, Barstow	7.3	36.0	3.20	79.98	412.98
LA13	Northridge, 1994, Newhall	6.7	6.7	1.03	59.98	664.93
LA14	Northridge, 1994, Newhall	6.7	6.7	1.03	59.98	644.49
LA16	Northridge, 1994, Rinaldi RS	6.7	7.5	0.79	14.95	568.58
LA17	Northridge, 1994, Sylmar	6.7	6.4	0.99	59.98	558.43

is the inter-story drift at yield and, d_i is the inter-story drift coordinate of the first mode shape. The story height, required to define the inter-story drift ratios (%), is taken as 3 m. The frame has a uniformly distributed mass of 30.0 metric ton per story, and was designed to have a linear first mode shape. The dominant period was tuned to 0.5 s. The ensemble of ground motions consists of the LA13, LA14, LA16 and LA17 records (Somerville et al. 1997) as they led to the largest drifts. Table 1 presents important parameters of these ground motions as well as of ground motions used in the following case studies. The yield shear forces of the stories were then computed based on the maximum shear forces experienced by the structure (during elastic time history analyses using the selected ensemble) divided by 4 to account for a load reduction factor of 4. A bi-linear hysteretic model with 2 % kinematic hardening was adopted to represent the behavior of the restoring shear forces.

The five story irregular structure of Fig. 2b is the second to be considered (termed "Irregular"). It was designed based on the regular shear frame previously presented. The stiffness of the first story was multiplied by a factor of 0.7 leading to a soft first story structure. Then all stiffnesses were scaled proportionally such that the fundamental period of the structure

Table 2 Monte Carlo simulation results for the regular shear frame

	Regular 0.5 %		Regular 0.7 %		Regular 1.0 %		Regular 1.2 %	
	Damping (kN*s/m) (a)	Envelope drift (%) (b)	Damping (kN*s/m) (c)	Envelope drift (%) (d)	Damping (kN*s/m) (e)	Envelope drift (%) (f)	Damping (kN*s/m) (g)	Envelope drift (%) (h)
1st story	4,920	0.500	3,188	0.700	1,692	1.000	1,200	1.200
2nd story	3,328	0.500	1,975	0.700	532	1.000	253	1.200
3rd story	2,252	0.500	1,209	0.700	94	1.000	0	1.010
4th story	1,456	0.500	762	0.700	6	1.000	0	0.785
5th story	744	0.500	393	0.700	28	1.000	8	1.192
COV = 7 %	–	0.573	–	0.851	–	1.729		1.896
		(115 %)		(122 %)		(173 %)		(158 %)
COV = 10%	–	0.607	–	0.914	–	2.001		2.185
		(121 %)		(131 %)		(200 %)		(182 %)
COV = 15 %	–	0.665	–	1.039	–	2.422		2.609
		(133 %)		(148 %)		(242 %)		(217 %)
COV = 0 %	–	0.520	–	0.725	–	1.024		1.220
COVc = 5 %		(104 %)		(104 %)		(102 %)		(102 %)
COV = 7 %	–	0.574	–	0.846	–	1.724		1.933
COVc = 5 %		(115 %)		(121 %)		(172 %)		(161 %)

remained at 0.5 s. In addition, the strengths of all stories except the first one were divided by 0.7 so that the first story was also weak. Here too, a bi-linear hysteretic rule with 2 % kinematic hardening was used to model the behavior of the shear restoring forces.

The third structure to be considered (termed "Regular2") is presented in Fig. 2c. As the "Regular" shear frame, it is also regular in elevation. Nonetheless, in contrast to the "Regular" shear frame its first mode shape is not linear in shape to eliminate specific sensitivity due to this property, if exists. The "Regular2" frame was also designed based on the "Regular" shear frame previously presented. The properties of the first two stories were taken as being equal to the properties of the first story of the "Regular" structure while the properties of the upper three stories were taken as being equal to those of the third story of the "Regular" structure. Its fundamental period was calculated as 0.47 s. Again, a bi-linear hysteretic rule with 2 % kinematic hardening was used to model the behavior of the shear restoring forces.

3.2.2 Optimal damping design

Optimal damping was designed for the three frames using the analysis/redesign procedure (Levy and Lavan 2006). The procedure was repeated for each example with 4 values of allowable drifts. These are 0.5, 0.7, 1.0 and 1.2 % of the story height. Those values were chosen to represent a broad range of possible values for design under the various seismic hazard levels in PBD. The optimal damping distributions and the corresponding envelope peak inter-story drifts are presented in the first five rows of Table 2 (Regular frame), Table 3 (Irregular frame) and Table 4 (Regular2 frame). Columns a and b list the damping and inter-story drifts for 0.5 % allowable drift. Also presented are corresponding values for −0.7 %

Table 3 Monte Carlo simulation results for the irregular shear frame

	Irregular 0.5 %		Irregular 0.7 %		Irregular 1.0 %		Irregular 1.2 %	
	Damping (kN*s/m) (a)	Envelope drift (%) (b)	Damping (kN*s/m) (c)	Envelope drift (%) (d)	Damping (kN*s/m) (e)	Envelope drift (%) (f)	Damping (kN*s/m) (g)	Envelope drift (%) (h)
1st story	6,363	0.500	4,498	0.700	3,075	1.000	2,469	1.200
2nd story	1,863	0.500	0	0.640	0	0.639	0	0.638
3rd story	1,118	0.500	0	0.500	0	0.512	0	0.527
4th story	785	0.500	0	0.633	0	0.614	0	0.627
5th story	484	0.500	80	0.700	0	0.886	0	0.899
COV = 7 %	–	0.602 (120 %)	–	0.949 (136 %)	–	1.107 (111 %)	–	1.225 (102 %)
COV = 10 %	–	0.654 (131 %)	–	1.095 (156 %)	–	1.256 (126 %)	–	1.339 (112 %)
COV = 15 %	–	0.744 (149 %)	–	1.395 (199 %)	–	1.597 (160 %)	–	1.584 (132 %)

Table 4 Monte Carlo simulation results for the regular2 shear frame

	Regular2 0.5 %		Regular2 0.7 %		Regular2 1.0 %		Regular2 1.2 %	
	Damping (kN*s/m) (a)	Envelope drift (%) (b)	Damping (kN*s/m) (c)	Envelope drift (%) (d)	Damping (kN*s/m) (e)	Envelope drift (%) (f)	Damping (kN*s/m) (g)	Envelope drift (%) (h)
1st story	5,187	0.501	3,329	0.700	1,893	1.000	1,374	1.200
2nd story	3,446	0.500	1,864	0.700	318	1.000	64	1.193
3rd story	2,709	0.500	1,464	0.700	205	1.000	70	1.196
4th story	387	0.500	0	0.567	0	0.394	0	0.367
5th story	0	0.205	0	0.209	0	0.230	0	0.241
COV = 7 %	–	0.573 (115 %)	–	0.806 (115 %)	–	1.293 (129 %)	–	1.993 (166 %)
COV = 10 %	–	0.601 (120 %)	–	0.866 (124 %)	–	1.434 (143 %)	–	2.264 (189 %)
COV = 15 %	–	0.670 (134 %)	–	0.996 (142 %)	–	1.667 (167 %)	–	2.647 (221 %)

allowable drift (columns c and d), 1.0 % allowable drift (columns e and f), and 1.2 % allowable drift (columns g and h). Note that in practical design the values of the damping coefficients are likely to be adjusted and rounded.

3.2.3 Uncertainties considered

The story stiffness and strength of a shear frame model depend linearly on the flexural stiffness and strength of its columns. Thus, the COV values of story stiffness and strength

Table 5 COV values adopted for RC elements' properties

Parameter	fc—concrete strength	fy—steel strength	Ec—concrete modulus of elasticity	Es—steel modulus of elasticity	b—section width	d—section active depth
COV	15.0 %	5.5 %	6.67 %	6.0 %	2.0 %	2.0 %

are the same as the COV values of the flexural stiffness and strength of its columns. Note that shear frames are theoretical structures and do not consist of actual structural members. Nonetheless, the COV values of their stiffness and strength are taken similar to those of actual structural members to keep the same level of uncertainty as that of realistic frames. Hence, a study was conducted so as to evaluate these values for both RC and steel sections. With the COV values for the story stiffness and strength at hand, their statistical distributions could be attained while adopting the lognormal distribution with the nominal stiffness or strength attained in the previous section (see Fig. 2) as the mean.

The parameters affecting the strength and stiffness of a reinforced concrete section are the effective depth of the section, d, its width, b, the steel area, A_s, the concrete strength, f_c, and modulus of elasticity, E_c, as well as the steel yield strength, f_y, and modulus of elasticity, E_s. A literature survey was conducted for the purpose of estimating the coefficients of variation of these parameters (COV). Henriques et al. (2008) made use of average values of 33, 400 and 30,000 MPa for f_c, f_y and E_c, respectively. The corresponding coefficients of variation were 15, 5.5 and 6.67 %, respectively. In another study, Celarec and Dolšek (2010) adopted COV values of 20 and 5 % for f_c and f_y, respectively. It should be noted that other values for COV(f_c) (as high as 32 %) have been used in the literature (De Stefano et al. 2013; D'Ambrisi et al. 2013). They indicated that such values, and even higher (up to COV(fc) = 50 %) were reported by Cristofaro (2009) for buildings in the Tuscany region. As the effect of steel strength on the element strength is crucial, we also performed a survey using 101 laboratory tests from various projects in Israel (not shown). The average strength and its COV were calculated as 440 MPa and 4.8 %, respectively. Data regarding the coefficients of variation of the section width, its effective depth and steel area are hard to find. The coefficient of variation of the steel cover could range from 20 % (Padgett et al. 2010) to 45 % (Frangopol et al. 2004). Based on these values and a steel cover of 5 % the section depth, a value of 2 % for the COV of section effective depth seems reasonable. Steel area is a parameter whose quality is controlled at a high level. Therefore, uncertainty in this parameter was not directly considered in this study. Nonetheless, as will be seen later, various levels of uncertainty are considered at the element level. Hence, the uncertainty in steel area is indirectly accounted for. In view of the above, the average values and the COVs adopted in this study for RC elements are presented in Table 5.

The parameters affecting the strength and stiffness of an "I" steel sections are the flange width, B, and thickness, t_f, the web depth, D, and thickness, t_w, and the steel strength, f_y, and stiffness, E_s. The COV values for these parameters are adopted from Kala and Kala (2005) and are given in Table 6. Similar values were found by Montiel and Ruiz (2007); Braverman et al. (2001) and Padgett et al. (2010).

Based on the COV values given above, for the shear frames only, a Monte Carlo simulation was conducted at the section level to evaluate the COV of its stiffness and strength. For each set of values attained for the section properties in the simulation, the section flexural stiffness (EI) and yield moment (M_y) were evaluated. In turn, their statistical distributions were built.

Table 6 COV values adopted for steel elements' properties

Parameter	fy—yield strength	Es—modulus of elasticity	b—flange width	h—section depth	t—flange thickness	a—web thickness
COV	5.6 %	6.0 %	1.0 %	0.44 %	4.4 %	4.0 %

COV values of 5.7 and 6.6 % were obtained for the RC section flexural stiffness (EI) and yield moment (M_y), respectively. For the steel section, corresponding values of 6.6 and 7.0 % were obtained. It should be noted that the strength and stiffness were found to be correlated. This is expected and, in fact, well known (see e.g. Priestley et al. 2007). Hence, the columns' strength and their stiffness are assumed correlated, or, their yield displacements are assumed deterministic. Thus, in the shear frames, the uncertainty is reduced to a single parameter in each column.

In many cases all columns at a given story are made of the exact same materials (same batch of concrete and steel). Hence, the uncertainty is further reduced to a single parameter in each story, the story strength (and its corresponding stiffness). The strength of each story is assumed to be uncorrelated to the strength of other stories, although they may have similar probability distributions. These distributions are assumed to be Lognormal with the mean taken as the nominal value computed for the bare frame. Three cases are considered for each frame and allowable drift. For each case a different value is assumed for the coefficient of variation of story strength. Those are 7, 10 and 15 %. The value of 7 % is based on the Monte Carlo simulation for the yield moment of a section considering uncertainty in its dimensions and strength, as presented above. The larger values for the COV are considered for older buildings where the uncertainty in structural properties may be larger.

Viscous dampers are tested in the factory to verify that they produce the desired force-velocity relation. Yet, there are two main sources of inaccuracy/uncertainty. The one is the orifice design that may lead to a slightly different force—velocity relation than desired (e.g. $\alpha \neq 1$) as well as a slightly different damping coefficient. The other is the transducer tolerance that may lead to errors in the measurements themselves. In practice, each damper is tested and expected to have all force-velocity points measured within ± 10 % of the desired function while some points may be above the desired and some points may be below (Taylor 2012). Although the error may be a result of a slightly nonlinear force-velocity relation, in this work a linear force-velocity relation was assumed with a COV of 5 % for the damping coefficients.

3.2.4 Seismic performance of the frames considering uncertainty

A Monte Carlo simulation was used to assess the sensitivity of the structural response to variations in the structural parameters considered. The 3 rows of Tables 2, 3, 4 indicated by COV = 7 %, COV = 10 %, and COV = 15 % present the mean of the MEPISD, and its value as a percent of the allowable, for these three values of COV and no uncertainty in damping coefficients. Table 2 also presents results from two additional simulations, the first for zero uncertainty in structural properties and COV(c_d) = 5 % for the damping coefficients and the second with COV = 7 % and COV(c_d) = 5 %. The mean values of the MEPISD were attained as follows (see also Fig. 1): for each structure and damping 1,000 sets of values for the strength distributions (and damping distributions where applicable) were generated. Each set included a value of strength (and damping) for each story. A nonlinear time history was then carried out for each set considering the whole ensemble of ground motions. The envelope

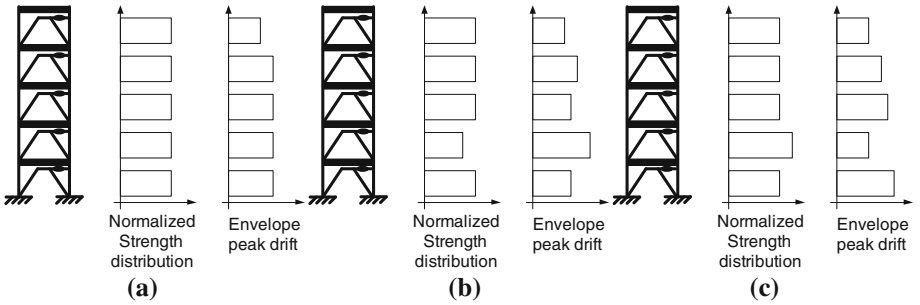

Fig. 3 Sensitivity of optimal designs

peak inter-story drift of each story was then computed and the maximum value of all stories was taken. This resulted in 1,000 values for the MEPISD, one for each set of strength and damping distributions among the stories. The mean of these 1,000 values is the one appearing in the table. It should be noted that for the sake of comparison a simulation with 10,000 sets of values for the strength distribution was carried out for the regular structure that was designed to 1.0 % drift. The results were almost identical to those obtained using 1,000 sets of values.

3.2.5 Discussion

As can be seen from the results presented in Tables 2, 3, 4, for all cases, the mean of the MEPISD considering structural uncertainty is larger than the MEPISD using nominal strengths. This can be attributed to the structure of the optimization problem. The constraint in the optimization problem is on the MEPISD or on the envelope peak inter-story drift of each story separately. This leads, in many cases, to equal drifts in many stories (as illustrated in Fig. 3a). In this case, a smaller strength (and stiffness) of a given story is expected to lead to a larger drift of that story and hence to a larger MEPISD than the allowable (Fig. 3b). A larger strength (and stiffness) of a given story, on the other hand, is expected to lead to a smaller drift of that story. However, it would usually lead to an increase in the drifts of adjacent stories. If the drifts of these stories using the nominal strength were equal to the allowable, the MEPISD would increase in this case too (Fig. 3c). That is, most variations in the structural strength (and stiffness) from the nominal values are expected to lead to an increase in the MEPISD.

This can also be seen from Fig. 4 which presents a histogram of the number of sets of strengths versus the MEPISD for the Irregular structure with allowable drift of 0.5 % and COV of 10 %. These results are typical for all cases.

The observation made above, and the insight gained, open the discussion on which designs are expected to be more sensitive to uncertainty in structural properties. Based on the above discussion it can be claimed that the sensitivity of the design is more pronounced when more stories reach the allowable drift, or close to it. This statement, however, is too general. Based on the results presented in Table 2 there seems to be another issue that strongly affects the sensitivity of a given design: the magnitude of the damping force in a story with respect to its yield shear. It is seen that when the damping force is relatively large, the sensitivity to uncertainty is limited (e.g. regular structure with 0.5 % allowable drift). This can be attributed to the smaller effect the story shear forces have on the maximum drift in the presence of large damping forces which dominate the structure's behavior. When the damping forces are relatively small, on the other hand, the effect the story shear forces have on the maximum

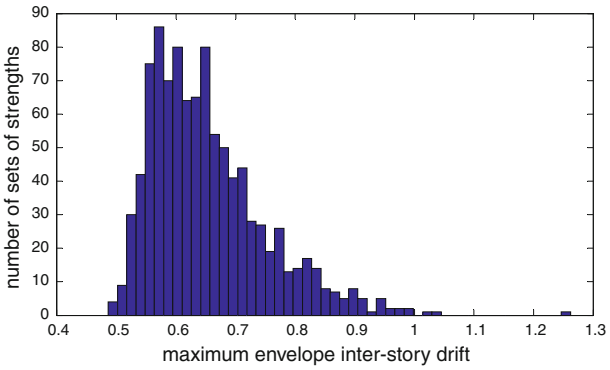

Fig. 4 Histogram of number of strength sets versus MEPISD for the irregular structure with allowable drift of 0.5 % and COV of 10 %

drift dominates. Hence, a very large sensitivity to uncertainty is observed in cases where the envelope peak inter-story drifts of some stories of the structure with nominal properties are close to the allowable, while the magnitude of damping forces in these stories is relatively small (e.g. regular structure with 1.0 % allowable drift). These stories will be termed "sensitive stories". This understanding can also explain why the sensitivity of the irregular structure is much smaller than that of the regular ones and why it is reduced as the allowable drift increases from 0.7 to 1.0 %. Of course, the larger the number of sensitive stories, the larger is the sensitivity of the structure.

Similar observations can be made regarding damping uncertainty with and/or without structural uncertainties. In all cases considered the mean of the MEPISD considering damping uncertainty is larger than the MEPISD using nominal damping. Nonetheless, the effect of damping uncertainty seems much smaller than the effect of structural uncertainty. This could be attributed to the fact that the sensitivity of the active constraints on drifts w.r.t infinitesimal changes in the design variables (damping coefficients) is zero at the optimum. In addition, the effect of damping uncertainty effect in cases were sensitive stories are present is smaller than in cases where there are no sensitive stories. This is because, by their definition, sensitive stories are stories with negligible or no damping. Hence, the effect of damping uncertainty in these stories is negligible. It can also be seen that the joint effect of structural and damping uncertainties is very similar to that of structural uncertainties only. Hence, in the following studies damping uncertainties are not considered.

3.3 Seismically designed steel moment resisting frame

3.3.1 Details of the bare frame, its modeling and the analysis tools

The second example adopts a plane model of the nine story control benchmark structure proposed by Ohtori et al. (2004). For the sake of simplicity spliced columns were replaced by continuous ones having the properties of the lighter section. In addition, all connections were assumed rigid while all columns had their strong axis resisting bending in the plane of the frame. The layout of the frame, as well as the cross sections used and floor masses, are presented in Fig. 5. The modulus of elasticity of steel was taken as 200,000 MPa while the yield strengths were taken as 345 and 248 MPa for the columns and beams, respectively. A secondary stiffness slope ratio of 2 % was assumed at the section level. The first natural period of the frame was calculated as 2.2 s.

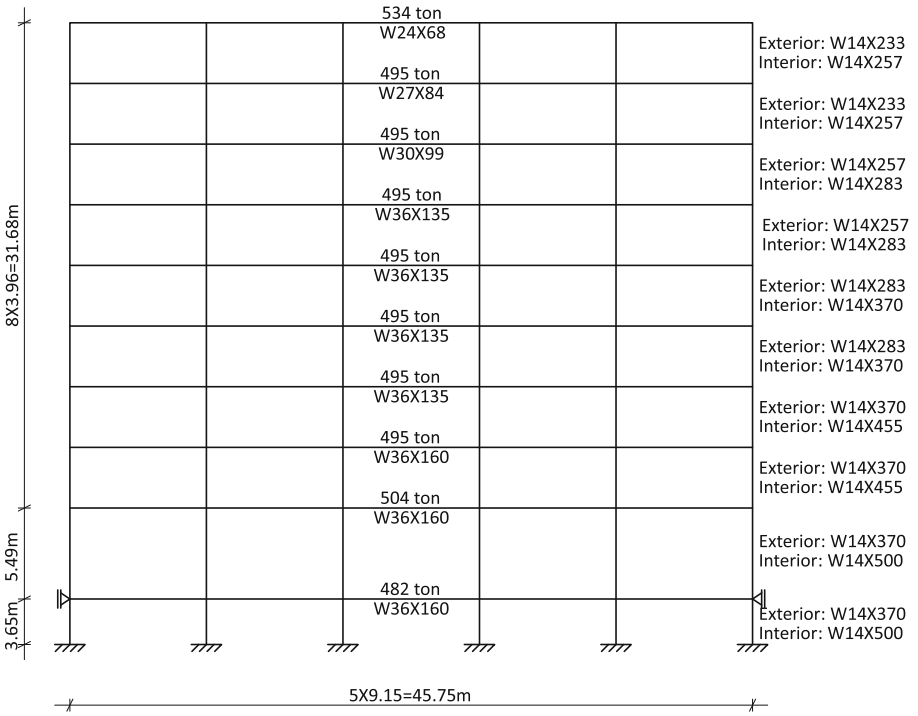

Fig. 5 Layout of the steel frame adapted from Ohtori et al. (2004)

The LA 10 % in 50 years ground motion records (Somerville et al. 1997) were scaled to fit the response spectrum at the site. The three records that led to spectral values closest to those of the design spectrum in the relevant periods were selected in this example (Fig. 6). These are LA04, LA06 and LA07. The following analyses were performed using the mixed lagrangian formulation (MLF) originally proposed by Sivaselvan and Reinhorn (2006) and modified by Sivaselvan et al. (2009) to enable an efficient analysis for large scale structures.

3.3.2 Optimal damping design

Optimal damping was designed for the structure using the analysis/redesign procedure (Levy and Lavan 2006) for allowable drifts of 0.5, 0.7, 0.9 and 1.0 % of the story height. The optimal damping distributions and the corresponding envelope peak inter-story drifts are presented in the first nine rows of Table 7. Columns a and b list the damping and inter-story drifts for an allowable drift of 0.5 %, columns c and d present the corresponding values for allowable drift of 0.7 %, and columns e through h present the corresponding values for allowable drift of 0.9 and 1.0 %. Again, in practical design the values of the damping coefficients are likely to be adjusted and rounded.

3.3.3 Uncertainty considered

In contrast to the shear frame examples, where each story was assigned with a single stochastic parameter, here the uncertainty is considered at the level of section dimensions and material

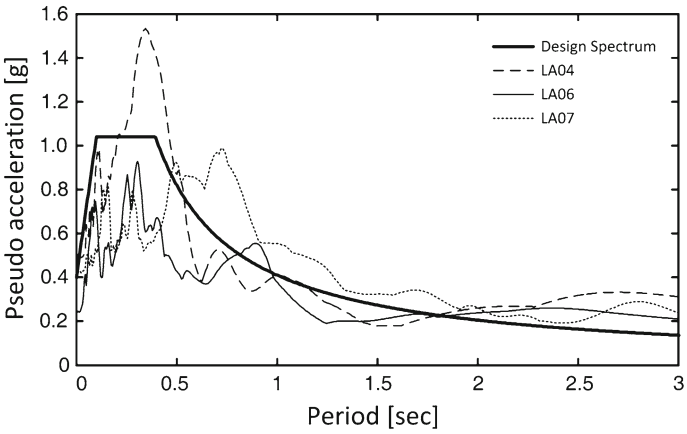

Fig. 6 Response spectrum considered for design and response spectra for the scaled LA04, LA06 and LA07 ground motions

Table 7 Monte Carlo simulation results for the steel frame

	Allowable drift 0.5 %		Allowable drift 0.7 %		Allowable drift 0.9 %		Allowable drift 1.0 %	
	Damping (kN*s/m) (a)	Envelope drift (%) (b)	Damping (kN*s/m) (c)	Envelope drift (%) (d)	Damping (kN*s/m) (e)	Envelope drift (%) (f)	Damping (kN*s/m) (g)	Envelope drift (%) (h)
1st story	10.89E4	0.5	7.31E4	0.7	4.33E4	0.9	3.04E4	1.0
2nd story	10.08E4	0.5	5.71E4	0.7	4.47E4	0.9	4.16E4	1.0
3rd story	7.03E4	0.5	3.03E4	0.7	1.73E4	0.9	1.32E4	1.0
4th story	10.60E4	0.5	6.45E4	0.7	4.27E4	0.9	3.53E4	1.0
5th story	5.59E4	0.5	0.85E4	0.7	0.34E4	0.9	0.04E4	0.986
6th story	4.97E4	0.5	1.74E4	0.7	0	0.861	0	0.914
7th story	3.13E4	0.5	0.79E4	0.7	0	0.863	0	0.923
8th story	2.69E4	0.5	0.75E4	0.7	0.17E4	0.904	0	0.947
9th story	0.28E4	0.5	0	0.587	0	0.72	0	0.750
Mean drift		0.54 (108 %)		0.801 (114 %)		1.0306 (115 %)		1.133 (113 %)
Median drift		0.539 (108 %)		0.799 (114 %)		1.0275 (114 %)		1.128 (113 %)
COV		0.9 %		2.5 %		3.1 %		3.4 %

properties. The COV values are taken as those of Table 6. The distributions are assumed to be Lognormal with the mean taken as the nominal value. As in the shear frame examples, it is assumed that all elements at a given story are made of the exact same materials.

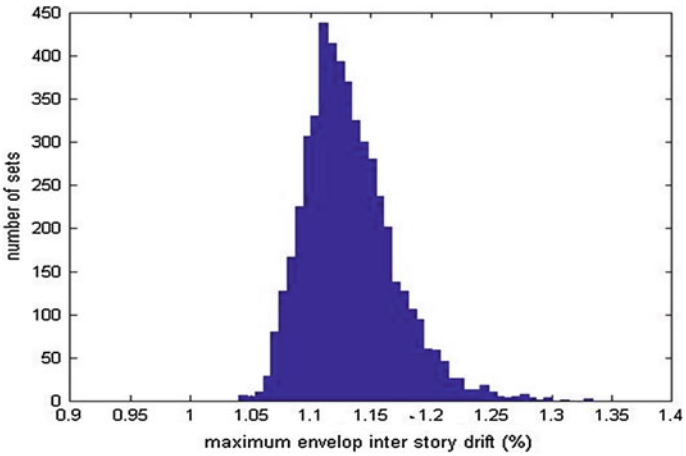

Fig. 7 Histogram of number of strength sets versus MEPISD for the steel frame with 1.0 % allowable drift

3.3.4 Seismic performance of the frame considering uncertainty in structural parameters

A Monte Carlo simulation was used to assess the sensitivity of the structural response to uncertainty in the structural parameters. The last three rows of Table 7 present the mean of the MEPISD, its median and COV. These are based on a population size of 1,000. For the sake of comparison, a simulation with 5,000 sets of values for the strength distribution was carried out for the structures designed to 1.0 % drift. The results were almost identical to those obtained using 1,000 sets of values.

3.3.5 Discussion

As can be seen, the results of this example show similar trends to the trends seen in the previous example. For one, the mean of the MEPISD considering uncertainty is larger than the MEPISD using the nominal properties. Again, this can be attributed to the structure of the optimization problem and also could be observed by plotting the histogram of the number of sets of strengths versus the MEPISD for 1.0 % allowable drift as an example (Fig. 7).

In addition, here too, the number of sensitive stories seems to affect the sensitivity to uncertainty. For example, the 5th to 8th stories in the design for 0.9 % drift are somewhat sensitive as the 5th and 8th stories reach the allowable drift and have small damping while the 6th and 7th stories have no damping and their drift is not much smaller than the allowable. This design indeed shows the largest sensitivity. On the other hand, the design for 0.5 % drift has a single sensitive story (the 9th story) and shows the smallest sensitivity.

It should be noted, on the other hand, that this frame is much less sensitive in comparison to the shear frames presented earlier. In the worst case (0.9 % allowable drift) the mean drift was 15 % larger than the allowable. Nonetheless, it should be kept in mind that this mean value represents a probability distribution function. For some strength distributions obtained in the Monte Carlo simulation the MEPISD was much higher (up to 35 % of the allowable). This can also be seen from Fig. 7. The mean + standard deviation of the MEPISD was circa 20 % larger than the allowable.

The fact that this frame is less sensitive than the shear frame can be attributed to several factors. It seems that the main reason is that a “weak story” mechanism is avoided. Hence, a

large inter-story drift in a single story is avoided. In fact, column yielding was not observed during the analyses while beam yielding was. In addition, "sensitive designs" having a large number of sensitive stories were difficult to generate. In most cases when one story with no damping attains a drift close to the allowable, other stories either have non-negligible damping or do not reach the allowable drift. Moreover, the effect of uncertainty in one location of flexural frames is smeared over several stories and its magnitude falls. Several factors contribute to that. For one, a "weak story" mechanism is avoided and the beams rather than the columns yield. Unlike the effect of column yielding in shear frames that is mostly local, the effect of beam yielding in flexural frames is distributed. Thus uncertainties in the values of their properties affect more than one story. Moreover, the stiffness of each story depends partially on the columns of the adjacent stories as these affect the rotational stiffness of the joints. Thus, the response of each story strongly depends on the properties of the beams and columns of adjacent stories. In such a case, the sensitivity to variations in the local properties is lower. Another point worth mentioning is that, in contrast to shear frames, yielding is gradual as not all elements in a story yield at the same time. Hence, a full mechanism in general, and a weak story mechanism in particular, are less probable.

3.4 Reinforced concrete frames

3.4.1 Details of the bare frames, their modeling and the analysis tools

The concrete frame structures considered are adopted from Seidel et al. (1989). These were designed per ACI 1983 for gravity only. In one of the structures the "strong column weak beam" rule is satisfied while in the other it is not. This allows investigating the influence that the relative beam strength (and stiffness) has on the sensitivity to uncertainty. The layout of the two frames is presented in Fig. 8a. The seismic mass per floor per resisting frame was taken as 222.2 ton for the "strong beam" structure and 181 ton for the "weak beam" structure and the periods of both structures were evaluated as 1.0 s. Cross sections through typical beams of the two structures are presented in Fig. 8b while their column properties are given in Table 8. The nominal stress-strain of the unconfined concrete and the steel are presented in Fig. 8c. Further details can be found in Seidel et al. (1989). The same ground motions used in the previous case study, namely LA04, LA06 and LA07 were adopted here too. In this case, however, each ground motion was scaled so as to lead to a 2 % maximum peak inter-story drift of the bare structure. The time history analyses for this case study were performed using IDARC (Park et al. 1987). A trilinear model was considered for the section moment-curvature relation that was assessed using a fiber model in IDARC.

3.4.2 Optimal damping design

Optimal damping was designed for both frames using the analysis/redesign procedure (Levy and Lavan 2006) with allowable drifts of 0.7, 1.1 and 1.3 % of the story height. Note that these are different than those used in the design of the steel frames for the following reasons: For one, at the level of drifts considered, damage to concrete frames is associated with higher levels of drifts (see e.g. FEMA 356, 2,000, table C1–3), and, in addition; The concrete frame could not be brought to smaller drifts without unrealistically large added damping. The optimal damping distributions and the corresponding envelope peak inter-story drifts are presented in the first six rows of Table 9. Columns a and b give the damping and inter-story drifts of the strong beam frame for an allowable drift of 0.7 % Columns c and d present the corresponding values for an allowable drift of 1.1 % and columns e through f present

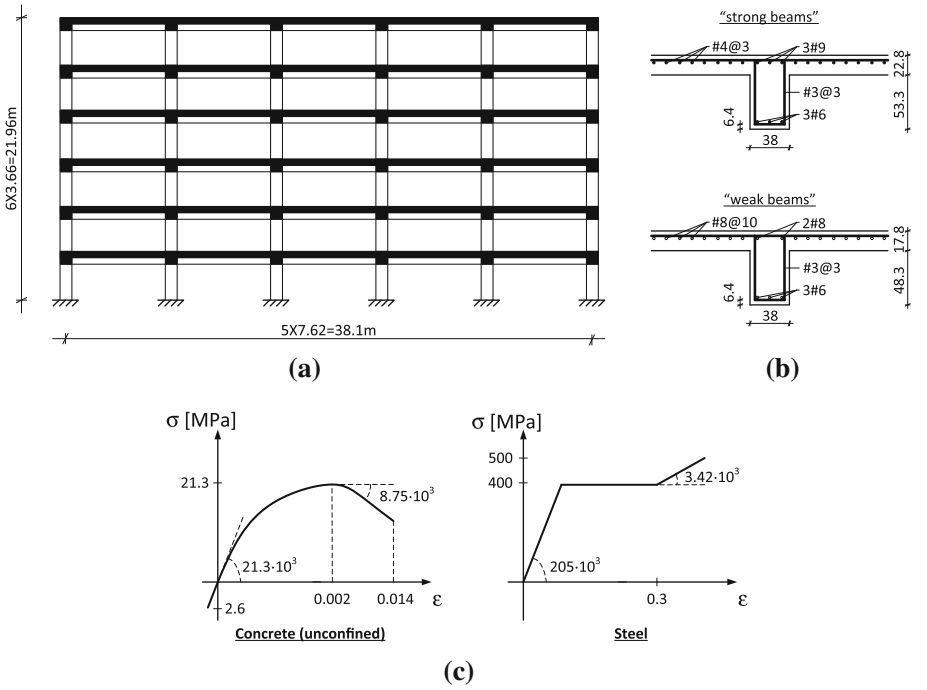

Fig. 8 The concrete frame structures adopted from Seidel et al. (1989): **a** layout **b** cross section of the beams in the strong beams and weak beams structures, and **c** stress-strain curves of the unconfined concrete and steel

Table 8 Column properties of the RC frames adopted from Seidel et al. (1989)

Story	Exterior			Interior		
	B [inch (cm)]	Reinforcement [US notation (mm^2)]	Ties [US notation (ϕmm@cm)]	B [inch (cm)]	Reinforcement [US notation (mm^2)]	Ties [US notation (ϕmm@cm)]
6	16 (40.6)	8#8 (1,520)	#3@16 (ϕ9.5@40.6)	16 (40.6)	8#8 (1,520)	#3@16 (ϕ9.5@40.6)
5	16 (40.6)	8#8 (1,520)	#3@16 (ϕ9.5@40.6)	16 (40.6)	8#8 (1,520)	#3@16 (ϕ9.5@40.6)
4	18 (45.7)	8#8 (1,520)	#3@16 (ϕ9.5@40.6)	18 (45.7)	8#8 (1,520)	#3@16 (ϕ9.5@40.6)
3	18 (45.7)	8#9 (1,924)	#3@18 (ϕ9.5@45.7)	20 (50.8)	6#14 (3,490)	#4@20 (ϕ12.7@50.8)
2	20 (50.8)	8#9 (1,924)	#3@18 (ϕ9.5@45.7)	24 (70.0)	8#14 (4,654)	#4@24 (ϕ12.7@70.0)
1	20 (50.8)	8#10 (2,374)	#3@20 (ϕ9.5@50.8)	24 (70.0)	8#14 (4,654)	#4@24 (ϕ12.7@70.0)

the corresponding values for 1.3 % allowable drift Corresponding values for the weak beam frame are presented in columns g–l. Again, in practical design the values of the damping coefficients are likely to be adjusted and rounded. It should be noted that for the frames to withstand such drifts, the shear capacity of the columns should be enhanced. Hence, it is assumed that, together with the addition of damping, measures to enhance the shear capacity of the columns were also taken (e.g. FRP jackets). These also assist in increasing the ductility capacity of the columns. It should be emphasized that although the strong beams frame was not designed according to the strong column weak beam practice, column yielding in the retrofitted frames was minor and in the worst case limited to two columns.

3.4.3 Uncertainty considered

As in the steel frame study, here too the uncertainty is considered at the level of section dimensions and material properties. Hence, the COV values are taken as those of Table 5. The distributions are assumed to be Lognormal with the mean at the nominal value. Again, it is assumed that all elements in a given story are made of the exact same materials.

3.4.4 Seismic performance of the frames considering uncertainty in structural parameters

A Monte Carlo simulation was used to assess the sensitivity of the structural response to uncertainty in the structural parameters. The last three rows of Table 9 present the mean of the MEPISD, its median and COV. These are based on a population size of 1,000.

3.4.5 Discussion

As can be seen, the results of this example show similar trends to those seen in previous examples. Again, the mean of the MEPISD considering uncertainty is larger than the MEPISD using nominal properties. Again, this can be observed by plotting the histogram of the number of sets of strengths against the MEPISD for the strong beams frame with, e.g., 0.7 % allowable drift (Fig. 9).

In addition, here too, the number of sensitive stories seems to affect the sensitivity to uncertainty. For example, the 1st and 6th stories in the strong beams frame designed for 0.7 % drift are somewhat sensitive as the 6th story reaches the allowable drift and has small damping, while the 1st story has no damping and its drift is not much smaller than the allowable. This design indeed shows the largest sensitivity.

It should be noted that, like the steel frame, these frames are less sensitive in comparison to the shear frames presented earlier. The reasons for this were discussed earlier. Note, however, that these frames are even less sensitive than the steel frame, when the mean inter-story drift is considered. This can be attributed to the smaller number of stories. Nonetheless, the COV associated with this mean drift is larger. Hence, for some strength distributions evaluated in the Monte Carlo simulation the MEPISD may be much (up to 58 %) higher than the allowable drift. This can also be seen from Fig. 9. The mean + standard deviation of the MEPISD reached a value approximately 20 % larger than the allowable, very similar to that of the steel frame.

Another point worth mentioning is the effect of the beam strength (and stiffness). Although column yielding was minor, the strong beams frame shows larger sensitivity to uncertainty, both in terms of the mean of the MEPISD and in terms of its COV. This can be attributed to the higher stiffness of the beams leading to a response which was more similar to that of the

Table 9 Monte Carlo simulation results for the RC frames

Story	Strong beams 0.7%		Strong beams 1.1%		Strong beams 1.3%		Weak beams 0.7%		Weak beams 1.1%		Weak beams 1.3%	
	Damping (KN s/m) (a)	drift (%) (b)	Damping (KN s/m) (c)	drift (%) (d)	Damping (KN s/m) (e)	drift (%) (f)	Damping (KN s/m) (g)	drift (%) (h)	Damping (KN s/m) (i)	drift (%) (j)	Damping (KN s/m) (k)	drift (%) (l)
1st	0	0.66	0	0.93	0	1.07	0	0.62	0	0.86	0	1.00
2nd	4.65E4	0.70	1.39E4	1.10	0.07E3	1.28	4.6330	0.70	1.76E4	1.10	9.08E3	1.30
3rd	1.48E4	0.70	0.06E4	1.09	1.11E3	1.30	1.9290	0.70	1.01E4	1.10	5.06E3	1.30
4th	1.41E4	0.70	0.54E4	1.10	3.66E3	1.30	1.2730	0.70	0.37E4	1.10	2.29E3	1.30
5th	0.57E4	0.70	0.19E4	1.10	1.43E3	1.30	0.3960	0.70	0.04E4	1.10	0.02E3	1.28
6th	0.05E4	0.70	0	0.61	0	0.54	0.0190	0.70	0	0.56	0	0.49
Mean drift		0.771 (110 %)		1.162 (106 %)		1.375 (106%)		0.750 (107 %)		1.165 (106 %)		1.371 (105 %)
Median drift		0.750 (107 %)		1.152 (105 %)		1.362 (105%)		0.741 (106 %)		1.152 (105 %)		**1.353** (104 %)
COV		8.45%		4.44%		4.74%		4.87%		4.86%		5.0%

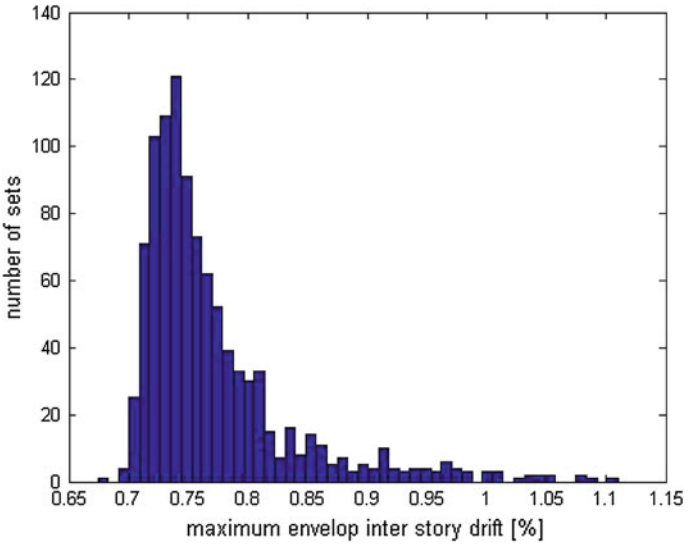

Fig. 9 Histogram of number of strength sets versus MEPISD for the RC strong beam frame with 0.7 % allowable drift

shear frames where the effect of uncertainty is more localized. However, in this frame the relative stiffness of the beams is not large enough to lead to sensitivity similar to that of the shear frames.

4 Conclusions and discussion

This paper examined the sensitivity of the response of optimally damped frames to uncertainty in structural and damping properties. In this study, it was assumed that the layout of the structure is known and that documentation in the form of structural plans is available. The uncertainty was limited to the level of element dimensions and material properties. It was shown that the MEPISD considering uncertainty is usually larger than that targeted based on nominal properties. This was attributed to the structure of the optimization problem. The constraint in the optimization problem is on the MEPISD. This leads, in many cases, to equal drifts in many stories. Hence, a smaller strength (and stiffness) of a given story is expected to lead to a larger drift of that story than the allowable. A larger strength (and stiffness) of a given story, on the other hand, is expected to lead to an increase in the drifts of the adjacent stories, potentially above the allowable. In other words, most variations in the structural strength (and stiffness) from the nominal values are expected to lead to an increase in the MEPISD.

In addition, it was seen that stories that reached or nearly reached the allowable drift in the optimal design, and in which the optimal damper is small or does not exist, are more sensitive to structural uncertainty. Furthermore, the larger the number of such sensitive stories in a design, the larger is the overall sensitivity. This is also the reason why vertically irregular frames seem less sensitive than regular ones.

In the shear frames, the effect of uncertainty in damper properties seemed to be small when the structural properties were taken as nominal. When uncertainty in both structural properties and damping were considered simultaneously, the results were very similar to

those obtained without damping uncertainty, especially in the sensitive designs. This could be attributed to the fact that the sensitivity of the active constraints on drifts w.r.t infinitesimal changes in the design variables (damping coefficients) is zero at the optimum. In addition, sensitive stories are the ones leading to sensitive designs. Sensitive stories, by definition, are stories with negligible or no damping. Hence, the effect of damping uncertainty in these stories on the overall sensitivity is negligible.

Although a large sensitivity was observed in the theoretical regular shear frames, its magnitude was smaller in realistic flexural structures. For the considered COV for structural properties, the flexural frames showed a mean of the MEPISD of up to 15 % larger than the target drift. For some strength distributions evaluated in the Monte-Carlo simulations the MEPISD may be much higher than the target drift (by up to 58 %). Nonetheless, these extreme values are highly improbable. The mean + standard deviation of the MEPISD reached a value approximately 20 % larger than the target. The lower sensitivity of flexural frames in comparison to the shear frames can be attributed mainly to the absence of a weak story mechanism. In addition, the influence of the strength and stiffness of the elements in one story on the displacements of another story smears the effect of uncertainty over several stories which lowers its magnitude. It should be kept in mind that the structural properties of one story were assumed to be uncorrelated with the structural properties of other stories. In small structures, this may not always be the case. Hence, in smaller structures smaller sensitivities may be expected.

References

Agrawal AK, Yang JN (1999) Optimal placement of passive dampers on seismic and wind-excited buildings using combinatorial optimization. J Intell Mat Syst Struct 10(12):997–1014

Attard TL (2007) Controlling all interstory displacements in highly nonlinear steel buildings using optimal viscous damping. J Struct Eng 133(9):1331–1340

Aydin E, Boduroglu MH, Guney D (2007) Optimal damper distribution for seismic rehabilitation of planar building structures. Eng Struct 29:176–185

Ben-Haim Y (2001) Information-gap decision theory: decisions under severe uncertainty. Academic Press, London, UK

Braverman JI, Miller CA, Ellingwood BR, Naus DJ, Hofinayer CH, Bezler P, Chang TY (2001) "Structural performance of degraded reinforced concrete members", Paper 1178, Transactions, SMiRT 16. Washington DC

Celarec D, Dolšek M (2010) The influence of epistemic uncertainties on the seismic performance of RC frame building, paper no.534, 14ECEE, Macedonia

Chen YT, Chai YH (2011) Effects of brace stiffness on performance of structures with supplemental Maxwell model-based brace-damper systems. Earthq Eng Struct Dyn 40:75–92

Cheng FY, Pantelides CP (1988) Optimal placement of actuators for structural control. Buffalo, NCEER

Christopoulos C, Filiatrault A (2006) Principles of supplemental damping and seismic isolation. IUSS Press, Milan

Constantinou MC, Symans MD (1992) Experimental and analytical investigation of seismic response of structures with supplemental fluid viscous dampers. N. C. f. E. E. Research, Buffalo

Cristofaro MT (2009) Metodi di valutazione della resistenza a compressione del calcestruzzo di strutture in c.a. esistenti. PhD Dissertation. Università di Firenze

D'Ambrisi A, De Stefano M, Tanganelli M, Viti S (2013) Influence of the variability of concrete mechanical properties on the seismic response of existing RC framed structures. In: Lavan O, De Stefano M (eds) Geotechnical, geological and earthquake engineering 24. Springer Science + Business Media, Dordrecht (in press). doi:10.1007/978-94-007-5377-8-5-5

Dargush GF, Sant RS (2005) Evolutionary aseismic design and retrofit of structures with passive energy dissipation. Earthq Eng Struct Dyn 34(13):1601–1626

De Stefano M, Tanganelli M, Viti S (2013) On the variability of concrete strength as a source of irregularity in elevation for existing RC buildings: a case study. Bull Earthquake Eng. doi:10.1007/s10518/013-9463-2

Di Paola M, Mendola LL, Navarra G (2007) Stochastic seismic analysis of structures with nonlinear viscous dampers. J Struct Eng 133(10):1475–1478
Di Paola M, Navarra G (2009) Stochastic seismic analysis of MDOF structures with nonlinear viscous dampers. Struct Control Health Monit 16(3):303–318
FEMA 356 (2000) Prestandard and commentary for the seismic rehabilitation of buildings. Federal Emergency Management Agency, Washington
Frangopol DM, Brühwiler E, Faber MH, Adey B (eds) (2004) Life-cycle performance of deteriorating structures: assessment. design and management, ASCE (ISBN 0-7844-0707-X), Reston, Virginia, p 456
Fujita K, Yamamoto K, Takewaki I (2010) An evolutionary algorithm for optimal damper placement to minimize interstorey-drift transfer function in shear building. Earthq Struct 1(3):289–306
Fujita K, Takewaki I (2012) Robust passive damper design for building structures under uncertain structural parameter environments. Earthq Struct 3(6):805–820
Gluck N, Reinhorn AM, Gluck J, Levy R (1996) Design of supplemental dampers for control of structures. J Struct Eng 122(12):1394–1399
Hahn GD, Sathiavageeswaran KR (1992) Effect of added-damper distribution on the seismic response of buildings. Comput Struct 43(5):941–950
Henriques AA, Veiga JMC, Matos JAC, Delgado JM (2008) Uncertainty analysis of structural systems by perturbation techniques. Struct Multidiscip Optimiz 35(3):201–212
Hwang JS, Huang YN, Yi SL, Ho SY (2008) Design formulations for supplemental viscous dampers to building structures. J Struct Eng 134(1):22–31
Kala J, Kala Z (2005) Influence of yield strength variability over cross-section to steel beam load-carrying capacity. Nonlinear Anal Model Control 10(2):151–160
Kim J, Choi H et al (2003) Performance-based design of added viscous dampers using capacity spectrum method. J Earthq Eng 7(1):1–24
Lavan O, Levy R (2005) Optimal design of supplemental viscous dampers for irregular shear-frames in the presence of yielding. Earthq Eng Struct Dyn 34(8):889–907
Lavan O, Levy R (2006) Optimal peripheral drift control of 3D irregular framed structures using supplemental viscous dampers. J Earthq Eng 10(6):903–923
Lavan O, Dargush GF (2009) Multi-objective optimal seismic retrofitting of structures. J Earthq Eng 13:758–790
Lavan O, Levy R (2009) Simple iterative use of Lyapunov's solution for the linear optimal seismic design of passive devices in framed buildings. J Earthq Eng 13(5):650–666
Levy R, Lavan O (2006) Fully stressed design of passive controllers in framed structures for seismic loadings. Struct Multidiscip Optimiz 32(6):485–498
Levy R, Lavan O (2009) Quantitative comparison of optimization approaches for the design of supplemental damping in earthquake engineering practice. J Struct Eng 135(3):321–325
Liu W, Tong M, Lee GC (2005) Optimization methodology for damper configuration based on building performance indices. J Struct Eng 131(11):1746–1756
Lopez Garcia D, Soong TT (2002) Efficiency of a simple approach to damper allocation in MDOF structures. J Struct Control 9(1):19–30
Montiel MA, Ruiz SE (2007) Influence of structural capacity uncertainty on seismic reliability of building under narroe-band motions. Earthq Eng Struct Dyn 36:1915–1934
Ohtori Y, Christenson RE, Spencer BF, Dyke SJ (2004) Benchmark control problems for seismically excited nonlinear buildings. J Eng Mech 130(4):366–385
Padgett JE, Ghosh J, Ataei N (2010) Sensitivity of dynamic response of bridges under multiple hazards to aging parameters, 19th analysis and computation specialty conference. ASCE
Park YJ, Reinhorn A M, Kunnath SK (1987) IDARC: inelastic damage analysis of frame shear-wall structures, Technical Report NCEER 87–0008
Park JH, Kim J et al (2004) Optimal design of added viscoelastic dampers and supporting braces. Earthq Eng Struct Dyn 33:465–484
Politopoulos I, Sollogoub P (2005) Vulnerability of elastomeric bearing isolated buildings and their equipment. J Earthq Eng 9(04):525–546
Politopoulos I, Pham HK (2009) Sensitivity of seismically isolated structures. Earthq Eng Struct Dyn 38(8):989–1007
Priestley MJN, Calvi GM, Kowalsky MJ (2007) Displacement-based seismic design of structures. IUSS Press, Pavia, p 721
Seidel MJ, Reinhorn AM, Park YJ (1989) Seismic damageability assessment of R/C buildings in eastern US. J Struct Eng 115(9), ASCE
Shukla AK, Datta TK (1999) Optimal use of viscoelastic dampers in building frames for seismic force. J Struct Eng 125(4):401–409

Silvestri S, Trombetti T (2007) Physical and numerical approaches for the optimal insertion of seismic viscous dampers in shear-type structures. J Earthq Eng 11(5):787–828
Singh MP, Moreschi LM (2001) Optimal seismic response control with dampers. Earthq Eng Struct Dyn 30(4):553–572
Singh MP, Moreschi LM (2002) Optimal placement of dampers for passive response control. Earthq Eng Struct Dyn 31(4):955–976
Sivaselvan MV, Reinhorn AM (2006) Lagrangian Approach to Structural Collapse Simulation. Journal of Engineering Mechanics 132(8):795–805
Sivaselvan MV, Lavan O, Dargush GF, Kurino H, Hyodo Y, Fukuda R, Sato K, Apostolakis G, Reinhorn AM (2009) Numerical collapse simulation of large-scale structural systems using an optimization-based algorithm. Earthq Eng Struct Dyn 38:655–677
Somerville P, Smith N, Punyamurthula S, Sun J (1997) Development of ground motion time histories for Phase 2 of the FEMA/SAC steel project. Report No. SAC/BD-97/04 1997
Soong TT, Dargush GF (1997) Passive energy dissipation systems in structural engineering. Wiley, London
Taflanidis AA, Beck JL (2008) An efficient framework for optimal robust stochastic system design using stochastic simulation. Comput Methods Appl Mech Eng 198(1):88–101
Takewaki I (2009) Building control with passive dampers: optimal performance-based design for earthquakes. Wiley, Singapore
Takewaki I (1997) Optimal damper placement for minimum transfer functions. Earthq Eng Struct Dyn 26(11):1113–1124
Takewaki I, Ben-Haim Y (2005) Info-gap robust design with load and model uncertainties. J Sound Vib 288(3):551–570
Taylor D (2012) Personal communication
Trombetti T, Silvestri S (2007) Novel schemes for inserting seismic dampers in shear-type systems based upon the mass proportional component of the Rayleigh damping matrix. J Sound Vib 302(3):486–526
Whittle JK, Williams MS, Karavasilis TL, Blakeborough A (2012) A comparison of viscous damper placement methods for improving seismic building design. J Earthq Eng 16(4):540–560
Wu B, Ou JP, Soong TT (1997) Optimal placement of energy dissipation devices for three-dimensional structures. Eng Struct 19(2):113–125
Yang JN, Lin S, Kim JH, Agrawal AK (2002) Optimal design of passive energy dissipation systems based on H infinity and H2 performances. Earthq Eng Struct Dyn 31(4):921–936
Zhang RH, Soong TT (1992) Seismic design of viscoelastic dampers for structural application. J Struct Eng 118(5):1375–1392